

Single Solution Phase Conformation of New Antiproliferative Cembranes

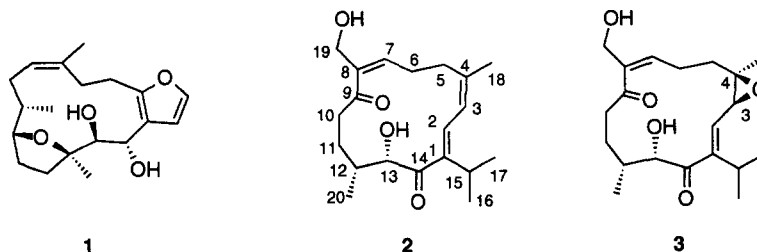
Angelo Fontana,* Maria Letizia Ciavatta, Pietro Amodeo and Guido Cimino

Istituto per la Chimica di Molecole di Interesse Biologico (ICMIB) del CNR, Via Toiano 6, 80072 Arco Felice, Napoli, Italy¹

Received 27 July 1998; revised 6 November 1998; accepted 19 November 1998

Abstract: Two new cembranes (**2** and **3**) have been isolated from the extract of the Antarctic sponge *Lissodendoryx flabellata*. Their structural elucidation has been performed by spectroscopic techniques, whereas the absolute configuration of the secondary carbinolic center was inferred by Mosher's method. The absolute stereochemistry of the second asymmetric carbon, as well as the solution conformation of **2**, has been determined by a computational approach based on conformational search, restrained molecular dynamics and *semi*-empirical calculations. The main product **2** showed cytotoxic and anti-proliferative activity against mammalian tumor cells. © 1999 Elsevier Science Ltd. All rights reserved.

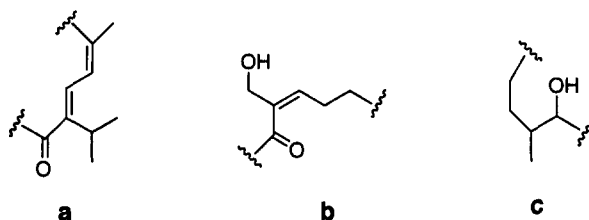
Chemical studies of cembranes, a large and various class of diterpenes isolated from terrestrial and marine sources,² have involved both X-ray and NMR elucidation of their medium sized ring. Accordingly, ten years worth of reports have produced a large database to assist the structural elucidation of new members of this class of natural products. Moreover, since the pioneering investigation of the tricyclic structure of pachyclavularolide (**1**),³ the biological and pharmacological effects⁴ of some cembranes have also encouraged conformational studies in solution.⁵ During our search of bioactive natural products, we have recently isolated from the apolar extract of the Antarctic sponge *Lissodendoryx flabellata* (Poecilosclerida, Myxillidae) two new cembranes (**2** and **3**) with very interesting activities against human cancer cell proliferation. Here we report the structures of flabellatene A (**2**) and B (**3**) and their topologic elucidation. The stereochemical assignment and the conformational analysis of the cytotoxic **2** were performed by using a combined approach of chemical methods and restrained molecular mechanics (MM) calculations and molecular dynamics (MD) simulations.



Results and Discussion

The sponge was collected and fractionated as described in the Experimental Section. Flabellatene A (**2**) was

Tel. +39 81 8534 156, Fax +39 81 8041770, E-mail: font@trinc.icmib.na.cnr.it;

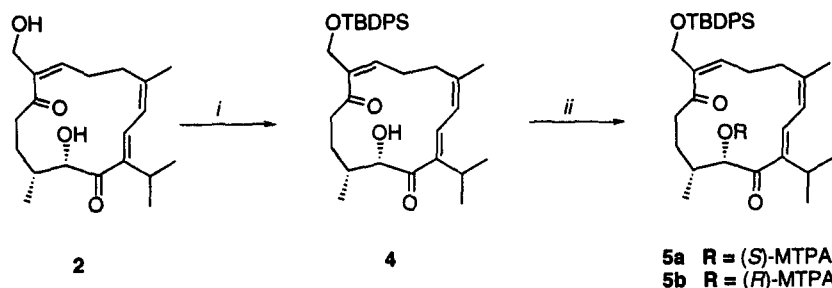


isolated as an amorphous white substance and had molecular formula $C_{20}H_{30}O_4$ as deduced by HRMS and ^{13}C -NMR data. The conjugated dienone moiety (partial structure **a**) was immediately established on the basis of the UV absorption at 293 nm, that well fitted both the IR absorptions (1668 and 1631 cm^{-1}) and the NMR values (Table 1). The assignment of the *iso*-propyl residue was made by comparison of the spectral data of **2** with those of other known cembranolides and confirmed by HMBC showing crosspeaks from H-15 to C-1, C-14 and C-2. Other IR (1703 and 3443 cm^{-1}) and ^{13}C -NMR (δ 206.0, 72.6 and 65.0) data indicated the presence of a further conjugated ketone and of two hydroxy groups. The relative positions of these moieties were determined on the basis of NMR spectra which allowed all resonances to be assigned and the fragments **b** and **c** to be drawn. In particular, the quaternary carbons at δ 206.0 (C-9) and 143.1 (C-8), and the vinyl proton at δ 5.76 (H-7) suggested a trisubstituted, conjugated double bond, as well as the downfield shift of the AB system at δ 4.50 and

Table 1. 1H - and ^{13}C -NMR Data of **2** and **3** in $CDCl_3$. Data are referred to internal $CHCl_3$ (δ 7.26 and 77.0) as internal standard.

	Compound 2			Compound 3		
	δ_H (mult, J (Hz))	δ_C	HMBC	δ_H (mult, J (Hz))	δ_C	HMBC
1	-	150.0 (s)	H-2, H-15	-	149.9 (s)	H-2, H-15
2	6.81 (<i>d</i> , 11.9 Hz)	135.0 (d)	H-15	5.71 (<i>d</i> , 9.4 Hz)	134.6 (d)	H-15
3	6.29 (<i>d</i> , 11.9 Hz)	120.6 (d)	H2-5	3.53 (<i>d</i> , 9.4 Hz)	58.3 (d)	-
4	-	139.6 (s)	H2-5, H3-18	-	63.5 (s)	H3-18
5	2.40 (<i>m</i>) 2.05 (<i>m</i>)	33.7 (t)	H-7	1.99 (<i>m</i>) 1.27 (<i>m</i>)	34.7 (t)	-
6	2.35 (<i>m</i>)	29.4 (d)	-	2.26 (<i>m</i>)	25.9 (t)	-
7	5.76 (<i>dd</i> , 14.7 and 4.0 Hz)	133.9 (d)	H2-19	5.75 (<i>dd</i> , 6.9 and 4.0 Hz)	135.2 (d)	H2-19
8	-	143.1 (s)	H-7, H2-19	-	141.9 (s)	H-7, H2-19
9	-	206.0 (s)	H-7, H2-10	-	206.0 (s)	H2-10
10	3.00 (<i>ddd</i> , 18.0, 2.9 and 1.5 Hz) 2.70 (<i>ddd</i> , 18.0, 2.9 and 1.5 Hz)	38.9 (t)	-	2.90 (<i>ddd</i> , 18.0, 7.0 and 2.0 Hz) 2.58 (<i>ddd</i> , 18.0, 2.9 and 1.5 Hz)	38.7 (t)	-
11	1.90 (<i>m</i>) 1.79 (<i>m</i>)	27.1 (t)	-	1.83 (<i>m</i>) 1.75 (<i>m</i>)	28.2 (t)	-
12	1.89 (<i>m</i>)	36.7 (t)	H-13, H3-20	1.74 (<i>m</i>)	35.5 (q)	H3-20
13	4.74 (<i>dd</i> , 5.8 and 1.1 Hz)	72.6 (t)	H2-20	4.57 (<i>bs</i>)	74.8 (d)	H2-20
14	-	202.8 (s)	H-15, H-13	-	203.9 (s)	H-15, H-13
15	3.10 (<i>m</i>)	27.8 (d)	H3-16, H3-17	3.03 (<i>m</i>)	28.8 (d)	H3-16, H3-17
16	1.15 (<i>d</i> , 6.9 Hz)	20.0 (q)	H-15	1.16 (<i>d</i> , 6.9 Hz)	20.0 (q)	H-15
17	1.24 (<i>d</i> , 6.9 Hz)	22.0 (q)	H-15	1.30 (<i>d</i> 6.9 Hz)	22.9 (q)	H-15
18	1.95 (<i>s</i>)	25.5 (q)	-	1.42 (<i>s</i>)	22.0 (q)	-
19	4.50 (<i>d</i> , 12.9 Hz) 4.25 (<i>d</i> , 12.9 Hz)	65.0 (t)	H-7	4.45 (<i>d</i> , 12.9 Hz) 4.25 (<i>d</i> , 12.9 Hz)	65.0 (t)	H-7
20	0.66 (<i>d</i> , 6.4 Hz)	12.8 (q)	H-13	0.68 (<i>d</i> , 6.3 Hz)	12.1 (q)	-

* Data marked by an asterisk are interchangeable.



Scheme 1. *i.* TBBDPSi chloride, DMAP in CH_2Cl_2 ; *ii.* (*R*)- or (*S*)-MTPA chloride, TEA, DMAP in CH_2Cl_2

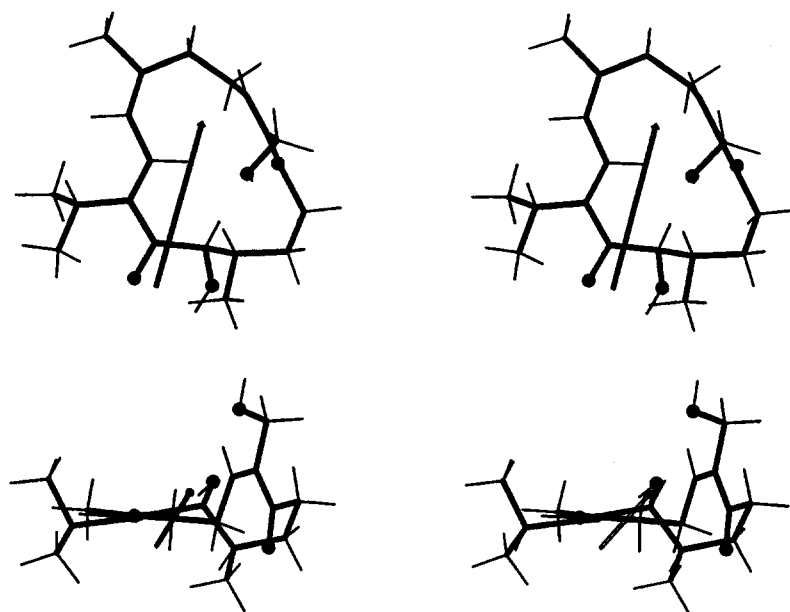
4.25 (H_2 -19) well agreed with the presence of the primary allylic alcohol. The correlations of H-7 with C-9 and C-8, in addition to that of this latter carbon with H_2 -19, led to the partial structure **b** which was completed by the COSY crosspeaks between H-7/ H_2 -6 (δ 2.35) and H_2 -6/ H_2 -5 (δ 2.40 and 2.05, H_2 -5). On the other hand, fragment **c** was built up on the basis of COSY and HOHAHA experiments which showed connectivities through the branched alkyl chain C10/C13. Finally, the HMBC correlations from C-4 to H_2 -5 and the methyl group at δ 1.95 (H_3 -18), as well as from C-9 to H_2 -10 and from C-14 to H-13, joined the single partial structures and gave the overall framework of **2**. The geometries of the conjugated systems in **2** were assigned on the basis of NOE and coupling constant data. In fact, a strong NOE between H-7 (δ 5.76) and both H_2 -19 led to the *Z* stereochemistry of C7/C8. On the other hand, NOEs between H-3 (δ 6.29) and H_3 -18 (δ 1.95) defined the *Z* geometry of C3/C4, as well as those ones between H-2 (δ 6.81) and H_2 -5 (δ 2.40 and 2.05) and between H-3 and H-15 (δ 3.10) suggested the *E* geometry of C1/C2 and the *S-trans* conformation of the conjugated diene. The depicted antiperiplanar conformation of the dienone was further supported both by the NMR values of the olefin carbons and by the coupling constant between H-2 and H-3 ($J = 11.9$ Hz), that is predicted to be smaller ($J = \text{ca. } 5.0$ Hz) in the *S-cis* form. Flabellatene A (**2**) has two chiral centers (C-13 and C-12). The protection of the primary alcohol with TBDPS (Scheme 1) followed by reaction of the product with (*R*)- or (*S*)-MTPA-Cl gave the corresponding Mosher's esters (**4a** and **4b**), of which $\Delta\delta$ analysis (Table 2) allowed one to attribute the *S* configuration at C-13 of **2**. Despite this, the assignment of the stereochemistry at C-12 proved to be much more complex. Some information could be gathered by the coupling constant between H-12 and H-13 ($J = 0.9$

Table 2 Selected^a $\Delta\delta$ (in ppm) of MTPA derivatives of cembranes **2** and **3**.

	Flabellatene A (2)			Flabellatene B (3)		
	$\delta_{S\text{-MTPA}}$ (5a)	$\delta_{R\text{-MTPA}}$ (5b)	$\Delta\delta$ (5a - 5b)	$\delta_{S\text{-MTPA}}$ (6a)	$\delta_{R\text{-MTPA}}$ (6b)	$\Delta\delta$ (6a - 6b)
H-12	2.16 (m)	2.21 (m)	- 0.05	2.07 (m)	2.10 (m)	- 0.03
H-20	0.81 (d)	0.88 (d)	- 0.07	0.84 (d)	0.90 (d)	- 0.06
H-10a	2.55 (m)	2.73 (m)	- 0.18	2.54 (m)	2.68 (m)	- 0.14
H-10b	2.45 (m)	2.60 (m)	- 0.15	2.43 (m)	2.55 (m)	- 0.12
H-3	6.29 (d)	6.28 (d)	+ 0.01	3.52 (d)	3.51 (d)	+ 0.01
H-15	3.06 (q)	3.04 (q)	+ 0.02	2.97 (q)	2.96 (q)	+ 0.01
H_3 -16	1.22 (d)	1.21 (d)	+ 0.01	1.31 (d)	1.30 (d)	+ 0.01
H_3 -17	1.15 (d)	1.14 (d)	+ 0.01	1.17 (d)	1.16 (d)	+ 0.01

^a Data were recorded in CDCl_3 by a 500 MHz spectrometer.

Figure 1. Stereo stick plot of the lowest energy conformer of **2**. Two mutually perpendicular views are shown. Bold lines are drawn for bonds involving only heavy atoms, while black balls are used for the four oxygen atoms. The central arrow represents the dipole moment vector of the molecule.



Hz), but a further elucidation of the structure was hampered by the scarce data available on the conformation(s) of cembrane's medium sized ring in solution. Fortunately, although lacking of any small ring, flabellatene's skeleton showed some extent of rigidity due to the presence both of the conjugated systems and of a hydrogen bond between the carbonyl oxygen at C-14 and the hydroxy group at C-13.⁶ Accordingly, NOESY experiments at different mixing times (between 200 and 1200 ms) gave a consistent pattern of qualitative and quantitative information.⁷ On the basis of their intensities, experimental NOEs (Table 3) were classified in two groups of distance ranges: 1.00 - 2.50 Å (strong effects) and 2.20-3.40 Å (weak effects). Whereby NOEs were unequivocally not observed, an "absent effect" was also introduced by considering an interprotonic distance longer than 3.5 Å (Table 3). Moreover, the dihedral angle between H-8 and H-9 was allowed to range from -120° to -80° or from 80° to 120° in agreement with the observed coupling constant ($J = 0.9$ Hz). These data, together with other significant coupling constants (Table 1), provided distance and angle constraints which were initially elaborated by a conformational search (CS) on all possible diastereoisomers of **2**. The two possible configurations at C12 led to 12*R* and 12*S* molecular model sets. Three structures were obtained in the 12*R* series, whereas no allowed conformation was found for the 12*S* chirality. Moreover, a full energy minimization (EM) collapsed the three 12*R* isomers to the single minimum shown in Figure 1. The finding of a single minimized structure, however, did not exclude the presence of equilibria between conformers with individual restraint violations, which could explain the experimental data. To rule out this hypothesis, restrained simulated annealing (SA) was run out. The systematic combination of the configuration at C12 with the conformation of the C8-C9 bond generated four sets of parameters corresponding to 12*R/S-trans*, 12*S/S-trans*, 12*R/S-cis* and 12*S/S-cis* isomers. Ten starting structures for each set were elaborated by several cycles of molecular dynamics (MD) and EM refinements. Once more, no ensemble for conformational subsets with the 12*S* configuration

Table 3. Selected distance ranges in Flabellatene A (**2**). Experimental data^a are correlated with those in the energetically minimized structure found by the *semi*-empirical calculations.

	Experimental distance in Å	Calculated distance in Å	Violation
H-2 / H-5 ^b	> 3.50 ^c	3.96	0.00
H-2 / H-6 ^b	2.20 - 3.40	2.99	0.00
H-2 / H-7	> 3.50 ^c	3.49	0.01
H-2 / H-12	2.20 - 3.40	2.63	0.00
H-2 / H-13	1.00 - 2.50	2.45	0.00
H-2 / H-19 ^b	> 3.50 ^c	4.47	0.00
H-3 / H-5 ^b	> 3.50 ^c	3.93	0.00
H-3 / H-6 ^b	> 3.50 ^c	4.65	0.00
H-3 / H-7	> 3.50 ^c	4.87	0.00
H-3 / H-15	1.00 - 2.50	2.16	0.00
H-3 - CH ₃ -18 ^b	2.20 - 3.40	2.77	0.00
H-10a / H-19b	2.20 - 3.40	3.25	0.00
H-11 ^b / H-19 ^b	> 3.50 ^c	5.34	0.00
H-13 / H-10a	2.20 - 3.40	3.00	0.00

^a Data were recorded in CDCl₃. ^c Absent effect.

fitted the experimental data. In particular NOEs between H-2 and H-12 and between H-2 and H-13 were never accounted for any combination of structures in the 12*S* chirality without large violation in other restraints. At the same time, the analysis of the 12*R* set gave an ensemble of structures that well explained the observed NMR values (Figure 2). It is noteworthy that this group contained the same structure found by CS calculations. In addition, no subset containing only *S-trans* conformation for the C8-C9 bond was able to fully account for the recorded spectra, whereas the *S-cis* conformation well agreed with the experimental constraints. To identify any bias induced by Tripos force-field⁸ on the calculated structure, this one was also refined with a semiempirical approach using the minimization option of the MOPAC package and different (AM1⁹ and PM3¹⁰) parametrizations. The starting conformation proved to be an energy minimum in all performed calculations, with only minor differences in geometrical parameters among the three minima, for which the best fit superimposition of the heavy atoms gives a root mean square (RMS) value of 0.25 Å. As a final check, the identified structure underwent a full unrestrained minimization, which resulted in only minor changes of the overall conformation

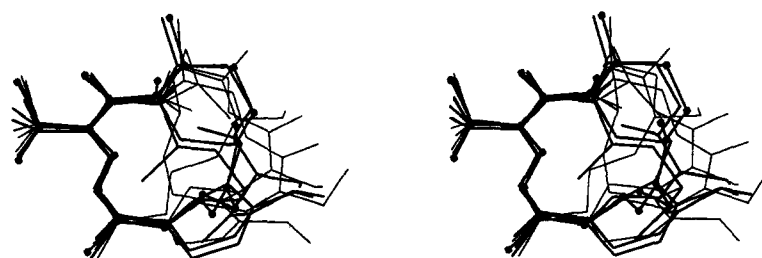


Figure 2. Stereo stick plot of a bundle of eight 12*R* calculated structures of **2**. The four most stable conformers for both 12*R/s-cis* (bold lines) and 12*R/s-trans* (thin lines) sets are shown. Small balls represent the atoms of the lowest energy conformer identified in the search. For clarity, hydrogen atoms are omitted.

(RMS = 0.18 Å). A check of the distance values corresponding to the experimental restraints showed only a minor violation (0.01 Å) associate to an absent NOE (Table 3).

The sponge extract contained a second cembranoid, flabellatene B (**3**), as a minor component. The spectral properties of **3**, [α]_D23 + 5.2° (c 0.5, CHCl₃), were very similar to those of **2**, except for the presence of an oxirane ring replacing the double bond C3/C4. Accordingly, the EIMS spectrum showed a highest peak at *m/z* 350 for the molecular formula C₂₀H₃₀O₅ (HREIMS *m/z* 350.4526), and the cembrane ring was featured by the ¹H-NMR signal at δ 3.53 (H-3) that matched the upfield shifts of H-2 (δ 5.71), H₂-5 (δ 1.99 and 1.27) and H₃-18 (δ 1.42). An intense NOE between this last methyl and the epoxide H-3 supported the *cis* geometry of the 3-membered ring, thus suggesting the formation of **3** by 1,2-*syn* addition of oxygen to the conjugated dienone in **2**. In agreement with this hypothesis, the determination of the absolute stereochemistry by Mosher's method confirmed the 13*S* configuration in **3** such as above reported for the main product **2**.

Conclusion

Among marine organisms, cembranes have been isolated from soft corals and molluscs.^{2a} The finding of flabellatene A (**2**) and B (**3**) may be the first example of this class of diterpenoid in sponges. It is noteworthy that the macroscopic analysis did not reveal any presence of symbionts in *L. flabellata*, although the origin from juvenile forms of soft coral inhabiting the sponge cannot be excluded. The combination of chemical, NMR and MM methods proved to be effective for the structure elucidation of **2**, including the absolute stereochemistry at C-12 and the *S-cis* conformation of the C7-C9 enone which could not be determined by a more traditional approach. Despite what is stated in other papers about the conformational analysis of cembranes, the flexibility of **2** did not spoil the MM endeavor. The single structure of **2** obtained from both CS and SA, without significant restraint violations, also resulted in the most stable isomer from an energetical point of view. This strongly supported the description of the observed NMR spectra in terms of a single conformer. Difficulties to obtain regular crystals of **2** at the moment do not allow any comparison with solid state conformation of this cembrane. A potentially interesting feature of the calculated structure derives from its charge distribution, that gives rise both to a rather large dipole moment (8.15 Debye, using the Gasteiger-Hückel charges¹¹), and to a typical long-range

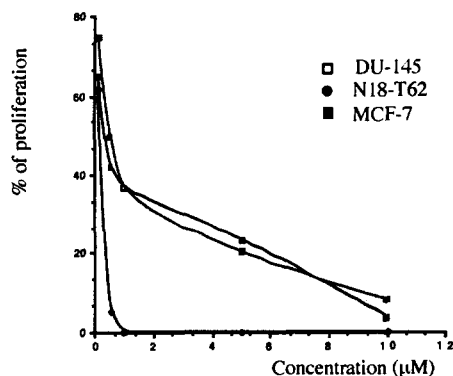


Figure 3. Cytotoxic and anti-proliferative effects of **2** against mammalian tumoral cells. Sample was added in EtOH to the multi-well dishes at the reported concentrations. Each analysis was performed in triplicates.

dipolar electrostatic field (Figure 1). In particular, the relative orientation of the carbonyl and hydroxyl groups leads to the concentration of the negative charge in the region surrounding C-13 and C-14, while the positive charge is more diffuse, spanning the hydrophobic region from C-3 to C-7. This charge distribution could account for the transport, mobility and recognition properties of the molecule in the biological action.

Flabellatene B (**3**) proved to be very similar to **2**. Although we could not demonstrate it experimentally, it is not farfetched to suggest that compound **3** shares the same stereochemistries and, very likely, the same preferred conformation of **2**.

Cembranes are known to affect cancer cell proliferation.^{5c-e} Therefore, we performed a series of preliminary experiments aimed at assessing whether flabellatene A (**2**) had potential antitumor properties.¹² This compound was cytotoxic on mouse neuroblastoma cells (N18-T62) at low concentrations (0.16 μ M), whereas significantly reduced cell proliferation of human tumoral cells (DU-145 and MCF-7) in a dose-depending manner (Figure 3).

Experimental Section

General Methods. Merck kieselgel 60 (70-230 Mesh) was used for silica gel chromatography and precoated kieselgel 60 F254 plates (Merck 0.25 mm precoated plates) were used for analytical TLC. NMR spectra were recorded on a Bruker WM-500 (500 MHz) and AMX 400 (400 MHz) spectrometers. Chemical shifts are reported in ppm referenced to CHCl_3 ($\delta=7.26$ for proton and 77.0 for carbon). Mass spectra were measured on a Carlo Erba TRIO 2000 VG instrument. IR spectra were recorded by a Bio-Rad FTS-7 spectrophotometer. Optical rotations were measured on a JASCO DIP-370 polarimeter. UV curves were obtained by a Varian UV-Visible spectrophotometer. NMR spectra were recorded using solutions of ca. 0.03 mM in CDCl_3 or C_6D_6 at 25° C. The resonance assignment of **2** and **3** was based on one- (^1H , ^{13}C , DEPT, NOED homodecoupling) and two- (COSY, HMQC, HMBC, TOCSY, NOESY) dimensional experiments. Spectra at variable temperature were recorded from 15° C up to 70° C in C_6D_6 , or from 15° C to 55° C in CDCl_3 . Semi-quantitative distances were calculated by NOESY experiments with mixing time at 200, 400, 600, 800 and 1200 ms.

Biological Material. The Antarctic sponge was collected at a depth of 70 m off Cape Russel (Antarctica, New Zealand) in January 1994. The sponge was classified as *Lissodendoryx flabellata* by Prof. M. Pansini at the University of Genova (Italy). In life the sponge was amorphous and red in colour. A taxonomic voucher specimen is deposited at the "Istituto di Zoologia" of the University of Genova (Italy).

Extraction and Isolation. The frozen sponge (12 g frozen weight) was extracted three times with acetone (3 x 200 mL). After removing the organic solvent, the aqueous suspension was diluted with fresh water (150 mL) and extracted first with diethyl ether (3 x 200 mL) and then with *n*-butanol (3 x 150 mL) to give ethereal (1.64 g) and butanolic (0.685 g) extracts, respectively. The ether soluble fraction (0.968 g) was chromatographed on Silica gel (Kieselgel 60, 100 g) using a petroleum ether/diethyl ether step gradient to give **2** (7.5 mg) and a mixture containing **3** as the major component. A further purification on reverse HPLC (column Merck Lichrosorb RP18, linear gradient from 30% up to 10% of H_2O in MeOH, Detector UV 254 nm, flow 3 ml/min) of the latest fraction gave **3** (3.5 mg).

Flabellatene A (2) [$\text{C}_{20}\text{H}_{30}\text{O}_4$] was obtained as a yellow oil (7.5 mg); $[\alpha]_D^{25} = -12.7^\circ$ ($c=0.3$, CHCl_3); UV (CHCl_3) λ_{max} ($\log \epsilon$) 293 (4080), 224 (2680), 205 (2920); IR (film) ν_{max} 3443 (OH), 2926-2867 (CH,

aliphatic), 1703 (C=O), 1668 (C=O), 1631, 1468, 1390, 1098; ^1H - and ^{13}C -NMR values, see Table 1; EIMS (m/z): 334 (2), 303 (10), 285 (5), 203 (55), 161 (60), 135 (100); HREIMS: m/z 334.4556 ($\Delta + 1.0$).

Flabellatene B (3) [$\text{C}_{20}\text{H}_{30}\text{O}_5$] was obtained as a yellow oil (3.5 mg); $[\alpha]_{\text{D}}^{20} = +5.2^\circ$ ($c=0.2$, CHCl_3); UV (CHCl_3) λ_{max} ($\log \epsilon$) 236 (7210); IR (film) ν_{max} 3442 (OH), 2974–2857 (CH, aliphatic), 1688 (C=O), 1571, 1473, 1390, 1083; ^1H - and ^{13}C -NMR values, see Table 1; EIMS (m/z): 350 (2), 332 (5), 285 (5), 301 (10), 275 (45), 261 (50), 166 (80), 139 (100); HREIMS: m/z 350.4526 ($\Delta - 1.4$).

Mosher's derivatives of 2. Under Argon, compound **2** (4 mg) was dissolved in dry CH_2Cl_2 (1 mL) and a catalytic amount of DMAP (N,N'-dimethylaminopyridine) was added under rapid stirring at room temperature. Then *tert*-butyldiphenylsilyl (TBDPS) chloride (3 drops) was added and the solution stirred for a further 2 h. When the starting material had been consumed (about 2 h as evidenced by SiO_2 -TLC with 15% Et_2O in petroleum ether), the solution was deposited on a TLC plate and chromatographed in light petroleum: Et_2O 85/15. The UV visible band (R_f 0.6) was scraped out and eluted with Et_2O to give 3.8 mg of TBDPS derivative **4**. This material was divided into two fractions, which were separately dissolved in dry CH_2Cl_2 (200 μL) and treated with a catalytic amount of DMAP and 30 μL of TEA (triethylamine). Under rapid stirring, (*R*)- or (*S*)-MTPA chlorides were added to each fraction. The reactions were kept for 12 h at room temperature, and then were fractionated by SiO_2 -TLC with 20% Et_2O in petroleum ether to give (*S*)-MTPA ester (**5a**; 0.8 mg) and (*R*)-MTPA-ester (**5b**; 1.2 mg), respectively.

Compound 4. Yellow oil (3.8 mg). ^1H -NMR (500 MHz, CDCl_3) δ : 7.64 (4H, m, TBDPS), 7.40 (6H, m, TBDPS), 6.79 (1H, d, $J = 11.9$ Hz, H-2), 6.29 (1H, d, $J = 11.9$ Hz, H-3), 5.61 (1H, bd, $J = 11.0$ Hz, H-7), 4.71 (1H, bd, $J = 6.2$ Hz, H-13), 4.51 (1H, d, $J = 13.0$ Hz, H-19), 4.25 (1H, d, $J = 13.0$ Hz, H-19), 3.05 (1H, q, $J = 7.0$ Hz, H-15), 2.87 (1H, ddd, $J = 18.0, 10.5$ and 2.0 Hz, H-10), 2.59 (1H, ddd, $J = 18.0, 8.1$ and 2.4 Hz, H-10), 2.32 (2H, m, H-6), 2.25 (1H, m, H-5), 1.98 (1H, m, H-5), 1.95 (3H, s, H-20), 1.86 (2H, m, H-11 and H-12), 1.71 (1H, m, H-11), 1.24 (3H, d, $J = 7.0$ Hz, H-16), 1.15 (3H, d, $J = 7.0$ Hz, H-17), 1.07 (9H, s, TBDPS), 0.66 (3H, d, $J = 6.2$ Hz, H-18).

Compound 5a. [(*S*)-MTPA ester] yellow oil (0.8 mg). ^1H -NMR (500 MHz, CDCl_3) δ : 7.63 (4H, m), 7.40 (10H, m), 6.80 (1H, d, $J = 11.6$, H-2), 6.28 (1H, d, $J = 11.6$, H-3), 5.78 (1H, bs, H-13), 5.63 (1H, bd, $J = 4.1$ Hz, H-7), 4.46 (1H, d, $J = 13.0$ Hz, H-19a), 4.22 (1H, d, $J = 13.0$ Hz, H-19b), 3.68 (1H, s, OCH_3), 3.06 (1H, m, H-15), 2.55 (1H, m, H-10a), 2.45 (1H, m, H-10b), 2.35 (2H, m, H-5a and H-6a), 2.16 (1H, m, H-12), 1.96 (2H, m, H-5b and H-6b), 1.94 (3H, s, CH_3 -18), 1.93 (1H, m, H-11a), 1.22 (3H, d, $J = 7.2$ Hz, CH_3 -16 or CH_3 -17), 1.15 (3H, d, $J = 7.2$ Hz, CH_3 -17 or CH_3 -16), 1.03 (9H, s, TBDPS), 0.81 (3H, d, $J = 7.0$ Hz, H-20).

Compound 5b. [(*R*)-MTPA ester] yellow oil (1.2 mg). ^1H -NMR (500 MHz, CDCl_3) δ : 7.62 (4H, m), 7.40 (6H, m), 6.81 (1H, d, $J = 11.4$, H-2), 6.28 (1H, d, $J = 11.4$, H-3), 5.84 (1H, d, 1.1 Hz, H-13), 5.63 (1H, dd, $J = 10.5$ and 5.1 Hz, H-7), 4.48 (1H, d, $J = 13.0$ Hz, H-19a), 4.24 (1H, d, $J = 13.0$ Hz, H-19b), 3.56 (3H, s, OCH_3), 3.04 (1H, m, H-15), 2.73 (1H, dd, $J = 17.7$ and 2.2 Hz, H-10a), 2.60 (1H, ddd, $J = 17.7, 7.5$ and 2.2 Hz, H-10b), 2.35 (1H, m, H-6a or H-5a), 2.27 (1H, m, H-5a or H-6a), 2.21 (1H, m, H-12), 1.98 (2H, m, H-5b and H-6b), 1.94 (3H, s, CH_3 -18), 1.93 (1H, m, H-11a), 1.58 (1H, m, H-11b), 1.21 (3H, d, $J = 7.2$ Hz, CH_3 -16 or CH_3 -17), 1.14 (3H, d, $J = 7.2$ Hz, CH_3 -17 or CH_3 -16), 1.03 (9H, s, TBDPS), 0.88 (3H, d, $J = 6.7$ Hz, CH_3 -18).

Mosher's derivatives of 3. As above described for **2**, 3.0 mg of flabellatene B (**3**) were transformed into the (*S*)-MTPA ester (**6a**; 0.8 mg) and (*R*)-MTPA-ester (**6b**; 1.0 mg).

Compound 6a. [(*S*)-MTPA ester] yellow oil (0.5 mg). $^1\text{H-NMR}$ (500 MHz, CDCl_3) δ : 7.73 (1H, m), 7.63 (3H, m), 7.41 (10H, m), 5.92 (1H, d, $J = 8.8$ Hz, H-2), 5.55 (1H, bt, $J = 8.4$ Hz, H-7), 5.45 (1H, s, $J = 1.6$ Hz, H-13), 4.39 (1H, d, $J = 13.0$ Hz, H-19a), 4.21 (1H, d, $J = 13.0$ Hz, H-19b), 3.62 (1H, s, OCH_3), 3.52 (1H, d, $J = 8.8$, H-3), 2.97 (1H, q, $J = 7.1$ Hz, H-15), 2.54 (1H, ddd, $J = 17.5$, 9.4 and 2.9 Hz, H-10a), 2.43 (1H, ddd, $J = 17.5$, 10.9 and 3.1 Hz, H-10b), 2.18 (2H, m, H_2 -6), 2.07 (1H, m, H-12), 1.95 (1H, m, H-5a), 1.64 (1H, m, H-11a), 1.42 (3H, s, CH_3 -20), 1.31 (3H, d, $J = 7.1$ Hz, CH_3 -16 or CH_3 -17), 1.27 (2H, m, H-5b and H-11b), 1.17 (3H, d, $J = 7.1$ Hz, CH_3 -17 or CH_3 -16), 1.02 (9H, s, TBDPS), 0.84 (3H, d, $J = 6.7$ Hz, H-20).

Compound 6b. [(*R*)-MTPA ester] yellow oil (1.2 mg). $^1\text{H-NMR}$ (500 MHz, CDCl_3) δ : 7.63 (4H, m), 7.41 (6H, m), 5.91 (1H, d, $J = 9.2$ Hz, H-2), 5.56 (1H, t, $J = 7.8$ Hz, H-7), 5.50 (1H, d, $J = 1.7$ Hz, H-13), 4.41 (1H, d, $J = 12.8$ Hz, H-19a), 4.22 (1H, d, $J = 12.8$ Hz, H-19b), 3.54 (3H, s, OCH_3), 3.51 (1H, d, $J = 8.8$ Hz, H-3), 2.96 (1H, q, $J = 7$ Hz, H-15), 2.68 (1H, ddd, $J = 17.2$, 9.0 and 3.0 Hz, H-10a), 2.55 (1H, ddd, $J = 17.2$, 8.3 and 3.2 Hz, H-10b), 2.20 (2H, bq, $J = 8.4$ Hz, H_2 -6), 2.10 (1H, m, H-12), 1.94 (1H, m, H-5a), 1.81 (1H, m, H-11a), 1.52 (1H, m, H-11b), 1.27 (1H, m, H-5b), 1.42 (3H, s, CH_3 -20), 1.30 (3H, d, $J = 6.8$ Hz, CH_3 -16 or CH_3 -17), 1.16 (3H, d, $J = 6.8$ Hz, CH_3 -17 or CH_3 -16), 1.03 (9H, s, TBDPS), 0.90 (3H, d, $J = 6.8$ Hz, CH_3 -18).

MM calculations. All molecular mechanics calculations were performed with Sybyl 6.2 package, by using the Tripos force-field and the Gasteiger-Hückel charge distribution. Semiempirical calculation were carried out with the Mopac 6.0 package.

The Gridsearch module of Sybyl was used for conformational search (CS). All $\text{C}(\text{sp}^3)\text{-C}(\text{sp}^3)$ and $\text{C}(\text{sp}^2)\text{-C}(\text{sp}^3)$ bonds were scanned with a 10° resolution. For the C7-C8 only the 0° and 180° conformations were sampled. The other $\text{C}(\text{sp}^2)\text{-C}(\text{sp}^2)$ bonds were kept fixed (see Discussion). Tolerances of 0.3 Å on bond length and 15 Å on valence angle were used for ring closure. Pseudo-atoms localized in the center of mass of H groups were used for restraints involving either magnetically equivalent, or not stereospecifically assigned protons. The simulated annealing (SA) procedure includes a 5 to 50 ps of molecular dynamics (MD) at a starting temperature varied in the range 500 to 1000 K, followed by a temperature lowering down to 200 K, with cooling rates from 10 to 50 K ps^{-1} . A time step of 1 fs and a heat bath coupling constant of 0.1 ps were used for all the SA runs. The Powell method was chosen for energy minimizations (EM), with a gradient norm convergence criterion of 10^{-4} kcal mol^{-1} Å $^{-1}$. Half-harmonic restraining potentials on distances and torsions were used both in SA and in EM, with force constant values of 5 kcal mol^{-1} Å $^{-2}$ (in SA), and 1 kcal mol^{-1} Å $^{-2}$ (in EM). Semiempirical calculations were carried with a MOPAC 6 program, using the AM1 and PM3 hamiltonians. The "precise" option was used for structure optimizations, which were performed in cartesian coordinates. Atomic point charges were calculated with the electrostatic potential approach.

Cytotoxicity and antiproliferative assays. MCF-7 (human breast adenocarcinoma) and N18-T62 (mouse neuroblastoma) cells were purchased from DMS (Germany), DU-145 (human prostate carcinoma) cells from ATCC (USA). Cell lines were cultured in dialyzed media prepared according to the instructions of the manufacturers. Cell proliferation assays were carried out in triplicates as described in ref. 12. Compound 2 was solved in EtOH and added 3h after cell seeding in six-well dishes (at a density about 10^4 cells/well). With DU-145 and N18-T62, trypsinized cells were counted by hemocytometer after 4 days. With MCF-7, the measurement was run after 5 days.

Acknowledgments. The authors wish to thank Dr. G. Villani, Miss D. Ricciardi, Mr. G. Scognamiglio and Mr. R. Turco for the technical assistance. We are grateful to Mrs. D. Melck for the biological assays. The NMR spectra were obtained from ICMIB NMR service, and mass spectra were from "Servizio di Spettrometria di Massa del CNR di Napoli ". Both staffs are acknowledged. This work was supported by the Italian National Research Program in Antarctica (PNRA) of CNR.

REFERENCES AND NOTES

1. Affiliated with the National Institute for the Chemistry of Biological Systems, CNR.
2. (a) Faulkner, D.J.; *Nat. Prod. Rep.* **1997**, *14*, 259 and references therein. (b) Hanson, J.R.; *Nat. Prod. Rep.* **1998**, *15*, 93.
3. Imman, W.; Crews, P.; *J. Org. Chem.* **1989**, *54*, 2526.
4. (a) Kobayashi, J.; Ohizumi, H.; Nakamura, H.; Yamakado, T.; Matsuzaki, T.; Hirata, Y.; *Experientia*, **1983**, *39*, 67. (b) Olsson, E.; Holth, A.; Kumlin, E.; Bohlin, L.; Wahlberg, I.; *Planta Med.*, **1993**, *59*, 293. For some informations about cytotoxic and antitumoral activities: (c) Rodrihuez, A.D.; Martinez, N.; *Experientia*, **1993**, *49*, 179 and references therein; (d) Govinidan, M.; Govinidan, G.N.; Kingston, D.G.I.; *J. Nat. Prod.*, **1995**, *58*, 1174 and references therein. (e) Yokomatsu, H.; Hiura, A.; Tsutsumi, M.; Satake, K.; *Pancreas*, **1996**, *13*, 154 and references therein.
5. (a) Berg, J.E.; Laaksonen, A.; Wahlberg, I.; *Tetrahedron*, **1991**, *47*, 9915. (b) Olsson, E.; Berg, J.E.; Wahlberg, I.; *Tetrahedron*, **1993**, *49*, 4975. (c) Vorobjev, A.V.; Sharikov, M.M.; Raldugin, V.A.; Heathcock, C.H.; *J. Org. Chem.*, **1995**, *60*, 63.
6. Joensten, M.D.; Schaad, L.J. In *Hydrogen Bonding*; Marcel Dekker, Inc., New York, **1974**; pp. 42-45.
7. Sanders, K.M., Hunter, B.K.; In *Modern NMR Spectroscopy*, Oxford University Press, Oxford, **1993**; 160-174 and references cited therein.
8. Clark, M.; Cramer III, R.D.; Van Opdenbosch, N.; *J. Comp. Chem.*, **1989**, *10*, 982.
9. Zoebisch, E.F.H.; Stewart, J.J.P.; *J. An.ºr. Chem. Soc.*, **1985**, *107*, 3902.
10. Stewart, J.J.P.; *J. Comp. Chem.*, **1989**, *10*, 221.
11. (a) Gasteiger, J.; Marsili, N.; *Tetrahedron*, **1980**, *36*, 3219. (b) Streitwieser, A.; *Molecular Orbital Theory for Organic Chemists*, **1961**, Wiley and Son, Ed., New York.
12. Simon, W.E.; Pahnke, V.G.; Holzel, F.; *J. Cin. Endoc. Metab.*, **1985**, *60*, 1243.